



IUCrData

ISSN 2414-3146

# X-ray diffraction images for two membrane protein crystals presenting high anisotropy; the *B. subtilis* ABC transporter BmrA and the *S. pneumoniae* NADPH oxidase

Veronica Zampieri,<sup>a</sup> Annelise Vermot,<sup>a</sup> Michel Thepaut,<sup>b</sup> Isabelle Petit-Hartlein,<sup>b</sup> Franck Fieschi,<sup>b,c</sup> Pierre Falson<sup>d</sup> and Vincent Chaptal<sup>d\*</sup>

Received 12 March 2025

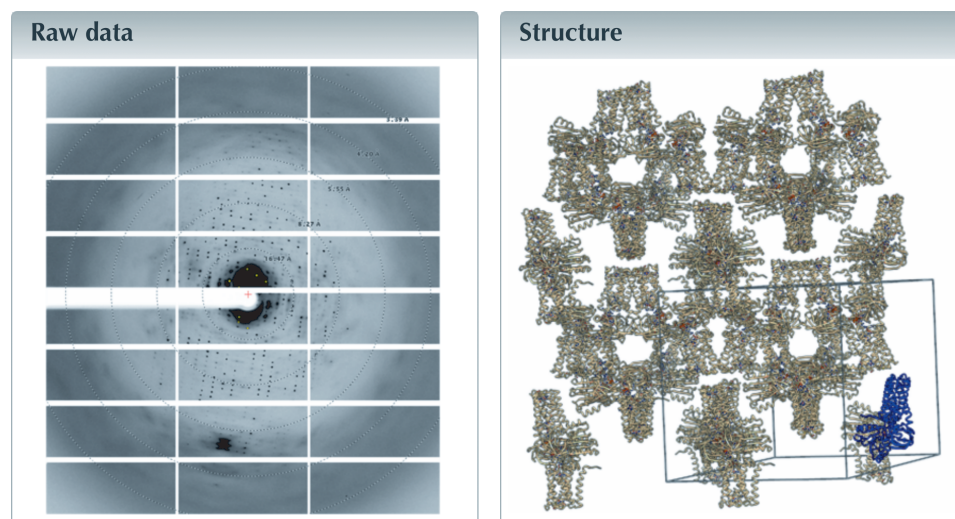
Accepted 30 June 2025

Edited by J. R. Helliwell, University of Manchester, United Kingdom

**Keywords:** membrane protein; diffraction anisotropy.

**Structural data:** full structural data are available from [iucrdata.iucr.org](https://iucrdata.iucr.org)

<sup>a</sup>EMBL Grenoble, 71 Avenue des Martyrs, Grenoble, France, <sup>b</sup>Univ. Grenoble Alpes, CNRS, CEA, Institut de Biologie Structurale, Grenoble, France, <sup>c</sup>Institut Universitaire de France, Paris, France, and <sup>d</sup>Molecular Microbiology & Structural Biochemistry, UMR5086, CNRS University Lyon-1, France. \*Correspondence e-mail: [vincent.chaptal@cnrs.fr](mailto:vincent.chaptal@cnrs.fr)



**HDF5 data files:** <https://doi.org/10.5281/zenodo.14894181>

**CBF data files:** <https://doi.org/10.5281/zenodo.14901515>

**Metadata imgCIF file:** <https://doi.org/10.1107/S2414314625005917/he4560img1.cif>

**Metadata imgCIF file:** <https://doi.org/10.1107/S2414314625005917/he4560img2.cif>

**Metadata imgCIF file:** <https://doi.org/10.1107/S2414314625005917/he4560img3.cif>

## Introduction

Diffraction anisotropy is a phenomenon more prevalently encountered with membrane protein crystals (Robert *et al.*, 2017), which results in artefacts in electron density maps making them difficult to interpret and prone to error in model building. Our previous study suggests that anisotropy would be linked to collinearity of secondary structure elements that cause stronger diffraction peaks in the 5 Å resolution limit area (Martin *et al.*, 2021). This collinearity of secondary structure elements is always observed in membrane proteins where *trans*-membrane segments are normal to the membrane plane. The data presented here (Table 1) are for two membrane proteins showing typical low

**Table 1**  
Experimental details.

Raw data	V-CK63-8-helical	V-CK63-8-ld	SpNox-Sp49-B3-B
DOI	<a href="https://doi.org/10.5281/zenodo.14894181">https://doi.org/10.5281/zenodo.14894181</a>	<a href="https://doi.org/10.5281/zenodo.14894181">https://doi.org/10.5281/zenodo.14894181</a>	<a href="https://doi.org/10.5281/zenodo.14901515">https://doi.org/10.5281/zenodo.14901515</a>
Data archive	Zenodo	Zenodo	Zenodo
Data format	HDF5	HDF5	CBF
Beamline	SOLEIL PX2	SOLEIL PX2	ESRF ID30
Detector	Eiger S 9M	Eiger S 9M	Pilatus3 2M
Radiation type	X-ray	X-ray	X-ray
Wavelength (Å)	0.9801	0.9801	0.9660
Beam centre (mm)	-111.2, 114.5	-111.2, 114.5	-130.2, 146.8
Detector axis	-Z	-Z	-Z
Detector distance (mm)	300.05	300.05	500.28
Pixel size (mm)	0.075 × 0.075	0.075 × 0.075	0.172 × 0.172
No. of pixels	3110 × 3269	3110 × 3269	1475 × 1679
No. of scans	1	1	1
Exposure time per frame (s)	0.025	0.025	1.7
Scan axis	$\omega$ , X	$\omega$ , X	$\omega$ , X
Start angle, increment per frame (°)	0.00, 0.10	0.00, 0.10	0.00, 0.20
Scan range (°)	360.00	360.00	260.00
No. of frames	3600	3600	1300
PDB code	6r72	–	8qq7

resolution and strong anisotropy that represented a major challenge in their structure solving. It is believed that the diffraction anisotropy present in the data is in fact the result of two unrelated phenomena. There is (i) a difference in resolution limits linked to the crystal packing that complicates the definition of a single resolution limit for the dataset, and (ii) a difference in intensity falloff in 3D compared to the empirical curve first described by Popov & Bourenkov (2003), leading to the idea that membrane proteins don't follow the empirical law derived from highly diffracting crystals of soluble proteins. The data presented here can be used by methods developers to test various hypotheses on how to handle such datasets.

### The *B. subtilis* multidrug ABC transporter BmrA

The inactive catalytic mutant E504A was used to trap the transporter in the outward-facing conformation in complex with ATP-Mg<sup>2+</sup>. The transporter is a homodimer and crystallized in the *P*<sub>2</sub><sub>1</sub> space group with two homodimers in the asymmetric unit. The solvent content is around 69%, typical for a membrane protein crystallized in detergent. The crystal that gave the highest resolution data was a large, long rod (Fig. 1). The crystal was illuminated using a microfocus beam on beamline PX2 (Duran *et al.*, 2013) at SOLEIL using two collection strategies. First it was collected at a single spot at 5% transmission for a low-dose data collection. This data set is included in the Zenodo deposition named 'V-CK63-8-ld\_1\_data\_xxxxx.h5'. Second, diffraction data were collected with a helical crystal translation strategy at nearly 100% transmission after moving the crystal so that the beam was hitting a different (previously unexposed) part of the crystal compared to the previous datasets; this data set is included in the Zenodo deposition named 'V-CK63-8-helical\_1\_data\_xxxxx.h5'. For information, by using a microfocus beam on such a large crystal we hoped to identify subdomains of better diffracting quality. Unfortunately, we were not able to identify any as judged by visual inspection of the diffraction patterns.

The structure of BmrA solved and refined using only the helical crystal translation data from this crystal has been published as part of the article by Chaptal *et al.* (2022), with a detailed material and methods section on structure solving and model building, which were challenging for this project.

### The *S. pneumoniae* NADPH oxidase

A F397W mutant of the *S. pneumoniae* NADPH oxidase (SpNOX) was crystallized with the *trans* membrane domain complexing two hemes and the dehydrogenase (DH) domain complexed with FAD. The full-length F397W SpNOX in detergent was crystallized as a monomer in space group *P*<sub>6</sub><sub>4</sub><sub>2</sub><sub>2</sub>

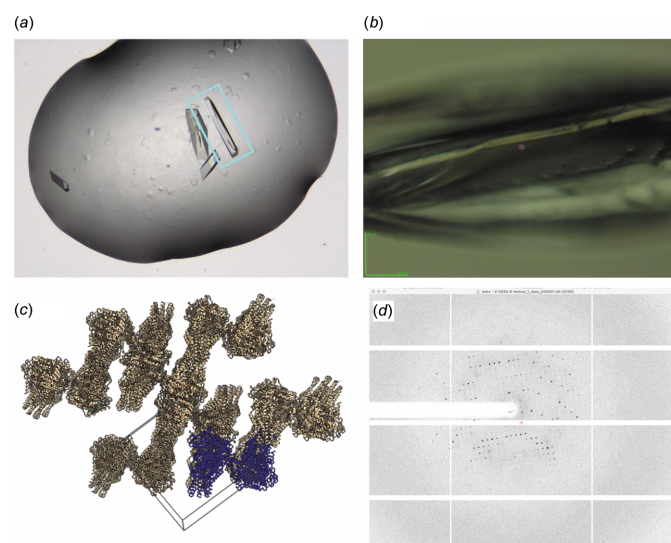


**Figure 1**  
ABC transporter BmrA. (a) A crystal in a hanging drop. The diffracting crystal is in the cyan rectangle. (b) The same crystal viewed from the PX2 beamline camera, probably before helicoidal data collection. (c) The crystal packing and unit cell. The asymmetric unit is shown in blue. (d) Typical diffraction image.

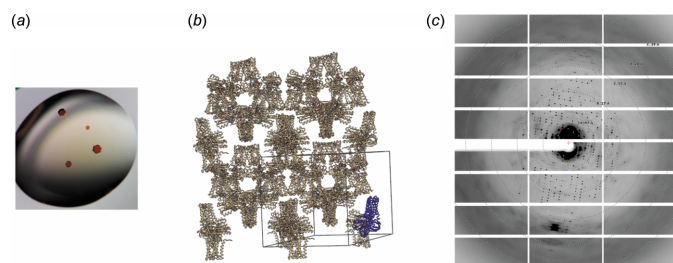


**Figure 2**  
NADPH oxidase SpNOX. (a) A typical spNOX crystal in hanging drops. (b) Crystal packing and unit cell for SpNOX. The asymmetric unit is shown in blue. (c) Typical diffraction image.

with a high solvent content of 76%. The typical crystal shape was a nice hexagonal firebrick (Fig. 2). More than 500 crystals were exposed to X-rays on the MASSIF-1 automatic beamline (Bowler *et al.*, 2015) at ESRF, Grenoble and 187 diffraction datasets were recorded and processed; among them only 32 reached resolutions better than 4 Å. A high-resolution structure is also available for the DH domain alone (<https://doi.org/10.2210/pdb8qq5/pdb>) (Petit-Hartlein *et al.*, 2024) that was used to solve our structure using molecular replacement. Two search models were used, first the DH domain was placed, then a model of the transmembrane domain made on the basis of multiple sequence alignment of NOX homologs and validated by structural alignment on CsNOX, another prokaryotic NOX (Magnani *et al.*, 2017). This high-resolution structure of the DH domain was also used during our model refinement as a reference template during model building. For the final refinement we used software dedicated to low resolution structures modelling, *ISOLDE* (Croll, 2018) and *LORESTR* (Kovalevskiy *et al.*, 2016) as described in the original paper (Petit-Hartlein *et al.*, 2024).

The structure of SpNOX solved and refined using data from this crystal was published as part of this article (Petit-Hartlein *et al.*, 2024), with a detailed material and methods section on structure solving and model building, which as mentioned above was challenging for this project.

### Funding information

This work was supported by the Centre National de la Recherche Scientifique (CNRS), Lyon University and the

Grenoble-Alpes University. VZ was supported by the Lyon-1 university EDISS doctoral school. This work was also supported by the French Agence Nationale de la Recherche Projects ANR-19-CE11-0023-01 for VZ, PF and VC, and ANR17-CE11-0013 to FF. The BmrA project benefitted from SFR Biosciences (Universite Claude Bernard Lyon 1, CNRS UAR3444, Inserm US8, ENS de Lyon) Protein Science Facility with the help of Virginie Gueguen-Chaignon, especially. The SpNOX work used the platforms of the Grenoble Instruct center (UMS 3518 CNRS-CEA-UJF-EMBL) with support from FRISBI (ANR-10- INSB-0502) and GRAL (ANR10-LABX-49-01) within the Grenoble Partnership for Structural Biology. AV was supported through the Emergence program from the University Grenoble Alpes.

### References

- Bowler, M. W., Nurizzo, D., Barrett, R., Beteva, A., Bodin, M., Caserotto, H., Delagenière, S., Dobias, F., Flot, D., Giraud, T., Guichard, N., Guijarro, M., Lentini, M., Leonard, G. A., McSweeney, S., Oskarsson, M., Schmidt, W., Snigirev, A., von Stetten, D., Surr, J., Svensson, O., Theveneau, P. & Mueller-Dieckmann, C. (2015). *J. Synchrotron Rad.* **22**, 1540–1547.
- Chaptal, V., Zampieri, V., Wiseman, B., Orelle, C., Martin, J., Nguyen, K. A., Gobet, A., Di Cesare, M., Magnard, S., Javed, W., Eid, J., Kilburg, A., Peuchmaur, M., Marcoux, J., Monticelli, L., Hogbom, M., Schoehn, G., Jault, J. M., Boumendjel, A. & Falson, P. (2022). *Sci. Adv.* eabg9215.
- Croll, T. I. (2018). *Acta Cryst.* **D74**, 519–530.
- Duran, D., Couster, S. L., Desjardins, K., Delmotte, A., Fox, G., Meijers, R., Moreno, T., Savko, M. & Shepard, W. (2013). *J. Phys. Conf. Ser.* **425**, 012005.
- Kovalevskiy, O., Nicholls, R. A. & Murshudov, G. N. (2016). *Acta Cryst.* **D72**, 1149–1161.
- Magnani, F., Nenci, S., Millana Fananas, E., Ceccon, M., Romero, E., Fraaije, M. W. & Mattevi, A. (2017). *Proc. Natl Acad. Sci. USA* **114**, 6764–6769.
- Martin, J., Robert, X., Gouet, P., Falson, P. & Chaptal, V. (2021). *bioRxiv* 2021.2012.2007.471609.
- Petit-Hartlein, I., Vermot, A., Thepaut, M., Humm, A.-S., Dupeux, F., Dupuy, J., Chaptal, V., Marquez, J. A., Smith, S. M. E. & Fieschi, F. (2024). *eLife* RP93759.
- Popov, A. N. & Bourenkov, G. P. (2003). *Acta Cryst.* **D59**, 1145–1153.
- Robert, X., Kassis-Sahyoun, J., Ceres, N., Martin, J., Sawaya, M. R., Read, R. J., Gouet, P., Falson, P. & Chaptal, V. (2017). *Sci. Rep.* **7**, 17013.